POLITECNICO
MILANO 1863

SCUOLA DI INGEGNERIA INDUSTRIALE
E DELL'INFORMAZIONE

Executive Summary of the Thesis

Critical assessment of RANS turbulence models in predicting the turbulent flow past a rectangular cylinder.

Laurea Magistrale in Aeronautical Engineering - Ingegneria Aeronautica

Author: Lorenzo Pierpaoli

Advisor: Prof. Maurizio Quadrio

Co-advisor: Dr. Alessandro Chiarini

Academic year: 2022-2023

1. Introduction

In this study the performance of four different turbulence models ($k-\epsilon$ (Launder *et al.*, 1975) (KE), Launder Sharma $k-\epsilon$ (Launder & Sharma, 1974) (LSKE), $k-\omega$SST (Menter, 1994) (KWSST) and Spalart-Allmaras with Zhang-Yang correction (Zhang & Yang, 2013) (SARC)) has been analyzed and compared to reference DNS results regarding the low Reynolds flow around a bluff body. The selected geometry is a rectangular cylinder of length L, thickness D and a ratio $L:D$ of 5. This geometry is indicated as the BARC benchmark and was introduced by Bruno *et al.* (2008) to develop an extensive database of simulations and experimental results regarding bluff body flows. Numerous studies, employing wind tunnels studies, LES, RANS and DNS simulations have been published since, covering a wide range of Re number and inflow conditions.
This flow is generally characterized by a complex structure comprised of large separated regions, flow reattachment and periodic vortex shedding. For this reason, despite its relatively simple geometry the BARC benchmark is particularly useful to assess the performance of different numerical methods and obtain useful informations that are of great interest for the world of civil and wind engineering. Given the complexity of this case the use of DNS simulations has become possible only in recent years and this flow at $Re = 3000$ has been the subject of two different studies: Cimarelli *et al.* (2018) and Chiarini & Quadrio (2021), with the latter being the reference solution considered for this study. The availability of a DNS solution allows for an improvement over the standard validation procedures of turbulence models based on the comparison to experimental results. Usually only quantities accessible through measurements like velocity profiles, pressure values or separation and reattachment points are considered for the the assessment of the ability of turbulence models. In this study, however, the complete knowledge of the flow offered by the DNS allows for the evaluation of the exact terms of the budget equation for the turbulent kinetic energy and the comparison of these terms to those computed through the use of the unsteady RANS simulations and different turbulence models. This approach allows for a more precise comparison and to observe which turbulent mechanisms and components of the TKE equation are predicted inaccurately by the turbulence models giving

useful information for the correction and developement of turbulence models.

2. Previous Studies and Flow Characteristics

In order to further discuss the BARC flow and its features the results of the latest DNS at $Re = 3000$ are here presented.

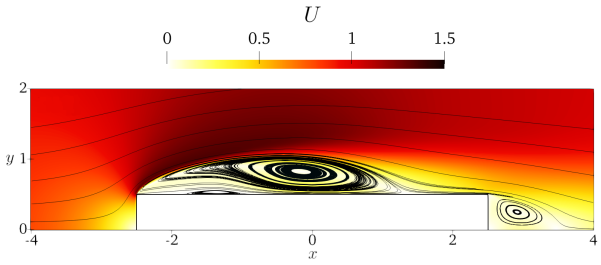

Figure 1: Mean streamlines drawn over a colormap of the magnitude of the mean velocity in the reference DNS simulation.

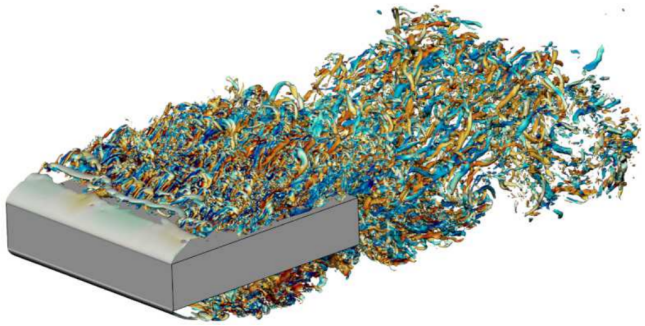

Figure 2: Instantaneous representation of isosurfaces with $\lambda_2 = -5$, coloring represents the value of streamwise vorticity ω_z, image taken from Chiarini *et al.* (2022)

Looking at the time averaged flow in figure 1 we can define two separated regions, originating from the leading and trailing edges. Inside the one originated by the LE interaction are located two vortices, the larger one, spanning from the leading edge to the reattachment point is indicated as the "Primary vortex" while the smaller one, placed upstream, near the wall, is indicated as the "Secondary Vortex", in the rear of the body, inside the second separated region is located the "Wake vortex". In Figure 2 the instantaneous flow gives us additional information to understand the formation and development of the recirculating regions: after the impingement on the front side of the cylinder the flow separates forming a laminar and bi-dimensional shear layer which then breaks down due to the Kelvin-Helmholtz instability into large spanwise vortices. The Kelvin–Helmholtz rolls are stretched by the mean flow and roll up generating hairpin vortices, further downstream the flow transitions in its turbulent state and the hairpin vortices break down in elongated streamwise vortices. This complex behaviour and the different features of this flow have attracted the attention of researchers and since 2008 numerous studies have contributed to the knowledge of this flow case, with a variety of different approaches. In Bruno *et al.* (2014) a review of the first four years of research is presented and decent agreement is observed for the resulting average drag coefficient $\langle C_d \rangle$ while a larger dispersion in the results is noted for the values of the root mean square of the lift coefficient $(C_l)_{rms}$, and for the length of the main recirculating region, additionally several studies present an unexpected average lift coefficient $\langle C_l \rangle \neq 0$ despite the complete symmetry that characterises this geometry. The cause of these unexpected results has been analyzed in several experimental and numerical studies in the following years focusing on different flow and geometry characteristics, such as: the effect of inaccuracy in the model shape for wind tunnel test and of its misalignment, inlet turbulence intensity, corner sharpness, pressure tap disturbances, mesh resolution and spanwise correlation. None of these studies unfortunately lead to conclusive results and are able to accurately explain the cause of the large dispersion of results that interests most of the studies regarding the BARC flow.

3. Numerical Methods

The reference solution utilized in this study is the DNS simulation of the flow at $Re_D = 3000$ from Chiarini & Quadrio (2021) where the Reynolds number is calculated using the thickness of the cylinder as the reference length, $Re_D = U_\infty D/\nu$ with U_∞ being the velocity imposed as a fixed value at the inlet and on the farfield wall, above and below the cylinder. In this simulation the incompressible Navier-Stokes equations are solved without any additional modelling on a staggered cartesian grid that extends in the stream-wise direction for $-22.5 < x < 40$, in the cross stream direction

for $-21 < y < 21$ and for $-2.5 < z < 2.5$ in the spanwise direction. The domain is discretized with $N_x = 1776$, $N_y = 942$ and $N_z = 150$ points in the three directions, for a total of over 250 million grid points, with varying spacing along the x and y direction in order to provide the highest resolution near the leading and trailing edges. The mean quantities are obtained exploiting temporal and ensemble averaging to achieve well converged values, with a total averaging time of $2345\frac{D}{U_\infty}$. Additional information regarding the DNS solution, the numerical schemes involved and the solver utilized are presented in Chiarini & Quadrio (2021). For the 2D URANS simulations the incompressible RANS equations are solved with the contribution of the four different turbulence models based on the Boussinesq hypothesis, the models were chosen for their frequent application in the industry field and in the case of the Launder Sharma model to evaluate the performance of a specific low Re model. The domain considered has the same extension of the DNS one in the x and y directions and maintain the same pattern of refinement with the smallest cells placed aorund the leading and trailing edges. For the KE, KWSST and SARC models three meshes have been considered to evaluate the grid independence of the results and they consist of 60758, 121920 and 245952 elements with a maximum y^+ value below one. In the case of the LSKE model three meshes consisting of 73924, 106108 and 145276 elements have been used with an average $y^+ \approx 0.8$. For the evaluation of the Re number effect the flow at $Re_D = 3 \times 10^5$ is simulated on three meshes of 33068, 212196 and 358322 elements and an average $y^+ \approx 10$. The equations are solved with the OpenFOAM software with a centered finite volume scheme and a Crank Nicholson time discretization method, the CFL number is kept always below 1 and the mean coefficients are obtained averaging over one period of the vortex shedding process.
The URANS simulations set up is presented in Figure 3, the boundary conditions applied to the domain elements are the following: at the inlet and at the farfield the value of k, ϵ, ω e $\tilde{\nu}$ are imposed, while at the outlet an homogeneous Neumann Boundary condition is applied. On the surface of the cylinder k and $\tilde{\nu}$ are imposed equal to zero, omega is imposed with the

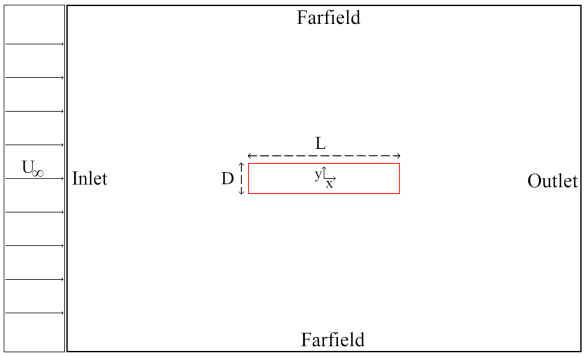

Figure 3: Simulation domain for 2D URANS

Menter's condition ($\omega_{wall} = \frac{6\nu_{wall}}{\beta_1 y^2}$, y indicates the height of the first cell) while for the dissipation rate a zero gradient boundary condition is imposed. The pressure is imposed at the outlet and calculated with a homogeneous Neumann condition at the farfield and inlet.

4. Results

The main analysis presented in this paper regards the flow simulations at $Re_D = 3000$, it focuses of the ability of the models to correctly identify the mean flow features, to evaluate the forces exerted on the cylinder body, to predict the correct velocity profiles and lastly to quantify the differences between the TKE budget terms. All results presented, when requiring the mean coefficients value, are obtained from the averaging in time of the flow over a period of the C_l oscillation that corresponds to 1 vortex sheddin1g cycle and varies for each turbulence model.

4.1. Mean Flow

The time averaged aerodynamic coefficients and the distribution of aerodynamic forces over the body surfaces are the first point of interest of this comparison. The reference solutions predicts an unsteady flow characterized by a vortex shedding frequency equal to $f = 0.1274$, a time averaged drag coefficient $\langle C_d \rangle = 0.9425$ and the root mean square of the lift coefficient equal to $(C_l)_{rms} = 0.29$. Out of the four models only the SARC is not capable of predicting the unsteady behavior of the flow due to the excessive damping of the wake shedding caused by the overestimation of the eddy viscosity in the rear region. The most accurate models in the prediction of the shedding frequency are the LSKE and

KWSST solutions, with a difference of 13.7% and 13.8% to the DNS case. These two model on the other hand exhibit the largest difference in the prediction of the mean drag coefficient compared to the DNS result with an error of +13.3% (LSKE) and +10.8% (KWSST), the best approximation is given by the KE model with an error of −1.2%. The value of the $(C_l)_{rms}$ is interested by a large variation among the models, this behaviour is expected given the results already in literature and described in Bruno *et al.* (2012), the KWSST and Launder Sharma model largely overpredict the variation of the lift coefficients with root mean square values of 0.856 and 0.741 respectively, in the case of the standard KE model this value is instead underpredicted with $(C_l)^{KE}_{rms} = 0.165$.

Another ability of the turbulence models that is assessed is the prediction of the correct turbulence structures that are formed in the mean flow. The two main elements of interest are the two recirculating regions originated by the flow interaction with the square corners of the cylinder and the inner structures that characterise them. In the reference solution the main recirculating region, that originates from the flow interaction with the leading edge, is constituted by the primary and secondary vortices. Of the four turbulence models considered, none are able to predict the existence of the secondary vortex, both the KWSST and KE models identify a large nearly elliptical primary vortex that extends from the LE to the reattachment point. The LSKE model predicts similarly only one vortex but it resembles more accurately the teardrop shape of the one identified in the reference solution. The SARC model also predicts only the primary vortex but its dimensions are consistently inferior than the expected solution. The primary vortex length predicted in the DNS is $L_1 = 3.95D$, the KE and its Launder Sharma variant are the more accurate in the prediction of this value with respectively $L_1 = 3.92$ and $L_1 = 4.01$. The LSKE model is also the most accurate in the prediction of the vortex center position, where the center is identified as the position in which $U = V = 0$. With regard to the wake vortex the KE model is overall the most reliable considering the vortex length and vortex center position prediction.

The forces exerted over the cylinder longitudinal sides by the flow have been analyzed observing the mean pressure $\langle c_p \rangle$ and wall shear stress $\langle c_f \rangle$ coefficients distribution over the body surface, that are rendered dimensionless with $\frac{1}{2}\rho U^2_\infty$. These coefficients are directly influenced by the flow structures that develop in the near wall region: the $\langle c_p \rangle$ remains negative over the whole longitudinal side with a nearly constant region corresponding to the secondary vortex, the primary vortex than induces a decrease of the coefficient due to the low pressure region related to the vortex center followed by a fast increase of pressure associated to the reattachment of the shear layer. The two equations turbulence models obtain comparable results in the upstream region of the cylinder with the KWSST and LSKE being the more accurate around the center of the body, downstream all the models are quite inaccurate (Fig. 4). The SARC model, given the different flow topology presents a very consistent difference compared to the reference solution.

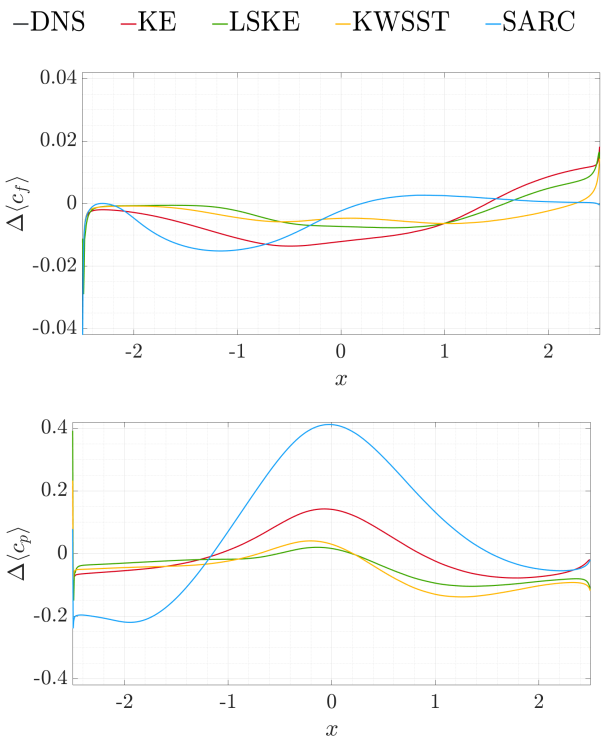

Figure 4: Friction and pressure coefficient difference between URANS and DNS solutions along the cylinder longitudinal side

.

The $\langle c_f \rangle$ distribution obtained from the DNS simulations presents a slightly positive region in the frontal part of the cylinder, a consequence

of the flow induced by the secondary vortex, the coefficient becomes negative in the region directly effected by the primary vortex and than slowly increases towards the trailing edge with the crossover point corresponding to the reattachment point. None of the model identify the presence of the secondary vortex and for this reason they are predicting a negative value of the coefficient in the front of the body. In figure 4 the difference between the coefficients computed by the turbulence model and the reference value is presented, in the first half of the cylinder the best approximation is achieved by the LSKE model while the SARC model offers the best performance in the rear part of the body. The accurate results of the SARC model are also noted in the comparison of the $\langle c_p \rangle$ profile over the cylinder backside in which this model performs better than all the others.
An additional comparison presented is the analysis of the velocity profiles computed in the vertical direction at four different location along the cylinder. These profiles aren't obtained at the same horizontal coordinate x for all the models but are instead computed at specific topological point of interest (Primary vortex center, reattachment point, trailing edge and wake vortex center) that are placed at different position among the models solutions. The difference to the same profiles obtained from the reference flow is computed showing that the Launder Sharma model offers the best result at the position of the primary vortex center and is comparable to the KWSST model at the reattachment point, while the SARC model is the most accurate at the trailing edge and at the wake vortex center.

4.2. Turbulent kinetic energy budget

The additional comparison proposed in this paper is the evaluation of the mean turbulent kinetic energy budget. The terms of the budget equation (total derivative, production, transport and dissipation of k) can be computed exactly with the reference results without the need to use any modelling, that is instead required when computing the budget terms' values for the URANS simulations. Starting from the distribution of kinetic energy in the flow field the reference solution identifies a region of $k \neq 0$ that extends along the shear layer starting from the leading edge, it corresponds to the laminar region of the shear layer. The transition to turbulent flow is coupled with the sudden increase in the value of k, that reaches a peak inside the primary vortex. The results presented by the turbulence models are quite different, the KE and KWSST models do not predict a laminar separation, the transitions is located at the leading edges and as a consequence a region of $k \neq 0$ develops along the shear layer and extends into the primary vortex. The LSKE model performs quite differently, with an unexpected region of $k > 0$ around the stagnation point in front of the cylinder, this phenomena has already been described by Durbin as the stagnation point anomaly. The increase of k in this region affects also the interaction with the leading edges leading to an increase of turbulent kinetic energy around these points. Despite these inaccuracies the performance along the shear layer in improved compared to the other turbulence models, with lower values of k and showing a similar result to the DNS case.

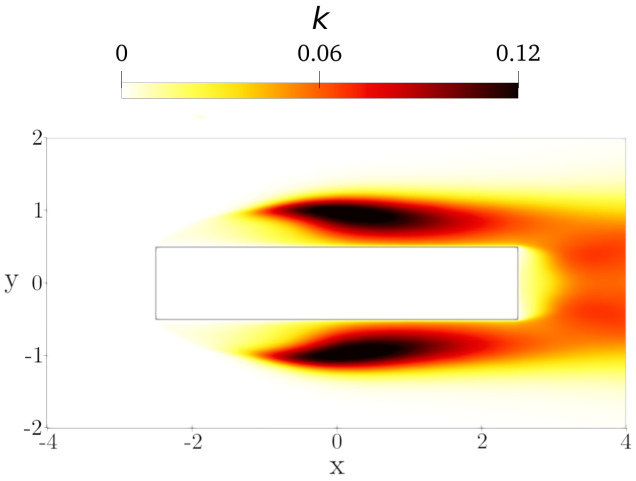

Figure 5: Distribution of k in the DNS solution

The ability to correctly predict the flow transition deeply affects the budget terms value, for the KWSST and KE models high values of production and dissipation are present along the shear layer, indicating an early transition of the flow after the interaction with the leading edges. The LSKE model presents instead inaccurate results in the LE region due to the stagnation point anomaly but offers a correct identification of the flow transition, denoted by the production term of k that is concentrated in the primary vortex and close to zero along the

shear layer. The difference between the budget terms value predicted by models and the reference ones has been evaluated at five topological point of interest (primary vortex center, peak of k, reattachment point, trailing edge and wake vortex center). The results among the models are comparable, with the LSKE model performing marginally better than the other models given its ability to predict more accurately the transition.

4.3. Turbulent inflow effect

The effect of incoming turbulence has been investigated imposing an inflow turbulence intensity of 5.7%. Similar studies have been presented reporting a reduction in the dimension of the recirculating regions proportional to the turbulence intensity. This results has been observed only in the case of the KE model in which the increase of turbulence models inhibits the vortex shedding mechanism and leads to a smaller primary vortex.

4.4. *Re* number effect effect

The effect of an increase in Re number, specifically up to $Re_D = 3 \times 10^5$, has been investigated with the KWSST and KE models. Compared to the low Re case a larger set of LES and experimental simulations are available for this flow condition. The increase of Re number has lead in previous studies to the upstream shift of the transition point with a consequent consistent production of k close to the leading edges. The URANS results are in line with the literature showing a region of non-null values of k spanning from the LE into the primary vortex center. The predicted drag coefficient is also in agreement with existing results, especially the KWSST model is quite accurate compared to the Wei and Kareem (2011) results at $Re = 10^5$. URANS simulations, given their limitations in the prediction of laminar shear layers, seem to be more suitable to this high Re flows in which the transition happens much closer to the leading edge.

5. Conclusions

The results shown in this study, regarding the performance of the four turbulence models considered in the simulation of the BARC flow, expose their limitations when dealing with low Reynolds number flows with such complex structures. The analysis of the turbulent kinetic energy budget, with the new approach introduced, indicates the turbulent mechanisms that these models fail to predict and thus giving useful information for the improvement of the turbulence models. The effect of the inflow conditions on the flow features, already assessed in literature, has been partially confirmed by the simulations conducted in this study. The simulations' accuracy dependence on Re number has been considered, the use of URANS simulations is more reliable in high Re cases.
This study offers a new approach in the evaluation and assessment of turbulence models, that coupled with the availability of high fidelity numerical solutions, could represent a useful tool for the researchers working on the development of new models, that are still of great interest given the prohibitive cost of LES and DNS simulations for industrial applications

References

Bruno, L., Coste, N. & Fransos, D. 2012 Simulated flow around a rectangular 5:1 cylinder: Spanwise discretisation effects and emerging flow features. *Journal of Wind Engineering and Industrial Aerodynamics* **104–106**, 203–215.

Bruno, L., Fransos, D., Coste, N. & Bosco, A. 2008 3D flow around a rectangular cylinder: A computational study. *Journal of Wind Engineering and Industrial Aerodynamics* **98** (6), 263–276.

Bruno, L., Salvetti, M. V. & Ricciardelli, F. 2014 Benchmark on the Aerodynamics of a Rectangular 5:1 Cylinder: An overview after the first four years of activity. *Journal of Wind Engineering and Industrial Aerodynamics* **126**, 87–106.

Chiarini, A., Gatti, D., Cimarelli, A. & Quadrio, M. 2022 Structure of turbulence in the flow around a rectangular cylinder. *Journal of Fluid Mechanics* **946**.

Chiarini, A. & Quadrio, M. 2021 The Turbulent Flow over the BARC Rectangular Cylinder: A DNS Study. *Flow, Turbulence and Combustion* **107** (4), 875–899.

Cimarelli, A., Leonforte, A. & Angeli, D. 2018 Direct numerical simulation of the flow around a rectangular cylinder at a moderately high Reynolds number. *Journal of Wind Engineering and Industrial Aerodynamics* **174**, 39–49.

Launder, B. E., Reece, G. J. & Rodi, W. 1975 Progress in the development of a Reynolds-stress turbulence closure. *Journal of Fluid Mechanics* **68** (3), 537–566.

Launder, B. E. & Sharma, B. I. 1974 Application of the energy-dissipation model of turbulence to the calculation of flow near a spinning disc. *Letters in Heat and Mass Transfer* **1** (2), 131–137.

Menter, F. R. 1994 Two-equation eddy-viscosity turbulence models for engineering applications. *AIAA Journal* **32** (8), 1598–1605.

Zhang, Q. & Yang, Y. 2013 A new simpler rotation/curvature correction method for Spalart–Allmaras turbulence model. *Chinese Journal of Aeronautics* **26** (2), 326–333.